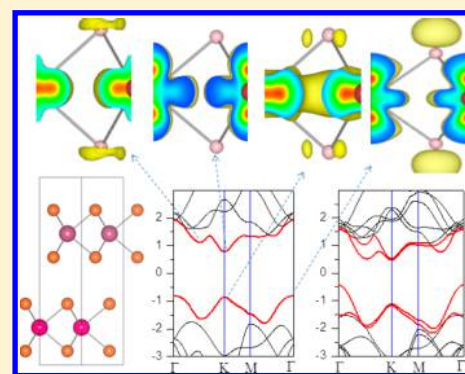


The Electronic Properties of Single-Layer and Multilayer MoS₂ under High Pressure

Xiaofeng Fan,^{*,†} C.-H. Chang,^{‡,§} W. T. Zheng,[†] Jer-Lai Kuo,[§] and David J. Singh^{*,†,||}[†]College of Materials Science and Engineering, Jilin University, Changchun 130012, China[‡]Department of Physics, National Taiwan University, Taipei 10617, Taiwan[§]Institute of Atomic and Molecular Sciences, Academia Sinica, Taipei, 10617, Taiwan^{||}Materials Science and Technology Division, Oak Ridge National Laboratory, Oak Ridge, Tennessee 37831-6056, United States

Supporting Information

ABSTRACT: We analyze the changes in the electronic structures of single-layer and multilayer MoS₂ under pressure using first-principles methods including van der Waals interactions. For single-layer MoS₂, the bond angle is found to control the electronic structure around the band gap under the pressure. For multilayer and bulk MoS₂, the changes in electronic structure under pressure are mainly controlled by the coupling of layers. Under pressure, the band gap of single-layer MoS₂ changes from direct to indirect, while multilayer MoS₂ becomes a band metal. Analysis of the real-space distribution of band-decomposed charge density shows that this behavior can be understood in terms of the different Mo d-electron orbitals making up the states near band gap including those at the top of valence band of Γ and K points and the bottom of conduction band along Λ and at the K point.



1. INTRODUCTION

Graphene, a honeycomb lattice carbon monolayer, has attracted enormous attention due to its fascinating physical properties and many potential applications, for example in energy storage.^{1–4} This has resulted in the intense interest in other two-dimensional (2D) materials, such as BN and transition-metal dichalcogenides.^{5,6} These 2D materials, like graphene, can be obtained with high crystal quality⁷ using micro-mechanical cleavage. MoS₂ has proven to be particularly interesting, both as a representative of the class of layered transition-metal dichalcogenides (TMDs) that is readily available and well suited for experimental study and due to properties that suggest potential application in electronic and optoelectronic devices.^{5,8,9}

Bulk MoS₂ is a highly anisotropic compound consisting covalently bonded layers that are stacked with weak van der Waals (vdW) interactions analogous to graphite.¹⁰ One of the main uses of MoS₂ is in dry lubrication, a characteristic that arises from the weak interlayer bonding. MoS₂ has also attracted interest due to catalytic activity of its crystal edges.¹¹ Turning to single layer MoS₂, prospective applications include field effect transistors with a large on–off ratio,^{12,13} applications of strong photoluminescence,⁸ and controllable valley and spin polarization,^{14,15} all of which have attracted both theoretical and experimental interest. Bulk MoS₂ is an indirect-gap semiconductor with a band gap of 1.29 eV,⁵ while going from bulk to single-layer, there is a transition from indirect to direct gap.⁵ Single-layer MoS₂ is found to have a direct band gap of approximately 1.8 eV.^{8,16} Various studies have addressed

modification of band gaps and photoluminescence in MoS₂ and the related group VI TMDs,^{17,18} for example, the use of strain-engineered MoS₂ monolayer for solar cells¹⁹ and the changes in electronic properties of MoS₂ and related materials induced by the strain.^{20–24} Mechanical strain modifies the band structure including both changes in the band gap and the carrier effective masses. The band gap of single-layer MoS₂ is even predicted to change from direct to indirect under large strain.²⁵ Recently, the photoluminescence of strained single-layer MoS₂ has been reported.²⁶ However, the microscopic physical mechanisms causing the changes in electronic structure and photoluminescence of MoS₂ under strain or pressure still needs further study, particularly regarding changes with the number of layers.

Pressure can be used as an effective parameter to analyze changes in band structures, as it is a clean variable, amenable to both experimental and first-principles study. In prior research, most work is focused on bulk MoS₂. Webb et al. reported the high-pressure behavior of bulk MoS₂ up to 5 GPa.²⁷ Aksoy et al. performed X-ray diffraction study of bulk MoS₂ to 38.8 GPa identifying a possible structural phase transition at about 25 GPa.²⁸ With the pressure up to 51 GPa, a 2H_v P63/mmc phase has been predicted near 26 GPa.^{29,30} It is interesting that structural phase transitions can occur in 2D monolayers of TMDs with mechanical deformations, as recently reported by

Received: January 12, 2015

Revised: April 25, 2015

Published: April 27, 2015

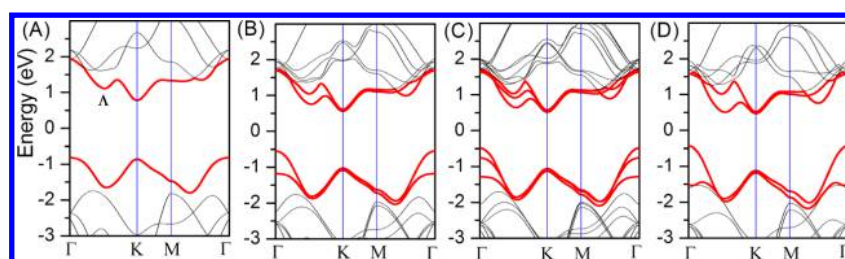


Figure 1. Band structures of single-layer (A), double-layer (B), three-layer (C), and bulk MoS₂ (D).

Duerloo et al.³¹ The pressure dependence of electronic properties, elastic constants, and structural properties of bulk MoS₂ have been investigated theoretically.^{32,33} However, while some experimental work on few layer MoS₂ has been reported,³⁴ theoretical predictions are lacking. Interestingly, a direct K–K to indirect Λ –K interband transition in bilayer MoS₂ was optically detected under hydrostatic pressure.³⁴

Here we present the changes under pressure in the band structure of MoS₂ with different numbers of layers based on first-principles calculations. The states near the band gap are from Mo *d*-electron orbitals. The important states near the top of valence band (TVB, we use this notation instead of “VBM” to emphasize *k*-dependence) and the conduction band bottom (BCB) at different *k*-points in the Brillouin zone are found to have very different real-space charge distributions. This is important for understanding the pressure dependence, as it leads very *k*-dependent response, and thus very strong distortions of the near gap band structure under pressure.

2. COMPUTATIONAL METHOD AND THEORETICAL MODEL

The present calculations are performed within density functional theory using accurate frozen-core full-potential projector augmented-wave (PAW) pseudopotentials, as implemented in the VASP code.^{35–37} We use the generalized gradient approximation (GGA) with the parametrization of Perdew–Burke–Ernzerhof (PBE)³⁸ with added van der Waals (vdW) corrections, which are important for describing the interaction between MoS₂ layers. These vdW interactions were included using the method of Grimme (DFT+D/PBE).³⁹ This approach has been successful in describing graphene-based structures.^{40,41} The *k*-space integrals and the plane-wave basis sets are chosen to ensure that the total energy is converged at the 1 meV/atom level. A kinetic energy cutoff of 500 eV for the plane wave expansion is found to be sufficient.

It is worth mentioning that quasiparticle (QP) methods including excitonic effects have been used for MoS₂.^{42–44} With many-body perturbation GW theory and a Bethe–Salpeter equation method, the quasiparticle band structures and optical properties can be studied, and were reported for monolayer MoS₂ by Shi et al.⁴⁵ and Qiu et al.⁴² The effect of spin–orbit coupling was also discussed for single-layer MoS₂.⁴⁶ Our band gap as obtained with the PBE/GGA is 1.65 eV, which is only slightly lower than the experimental value approximately 1.8 eV. The reported monolayer QP gap calculated by GW method is approximately 2.8 eV and the first excitonic peak in absorption spectra is about 1.9 eV with strong electron–phonon broadening in the visible and ultraviolet ranges.⁴² The strong excitonic effect is a consequence of the reduced screening and low effective dielectric constant in the monolayer. Clearly, the PBE band gap is an underestimate as in common in standard density functional calculations. Though the band gap is

underestimated by PBE, the band structure near the gap does not show obvious differences from that obtained by many body methods. It has *d*-electron character as the discussion below. It is expected that the origins of the response of band structure of MoS₂ to the pressure can be analyzed using PBE calculations.^{32,33} It would also be of interest to construct tight binding models, as was done previously for monolayer MoS₂.^{47–50} These are often useful in understanding band formation. For the pressure dependence, these would require the bond length dependent hopping and overlap matrix elements, as well as a pressure dependence of the onsite parameters.

Our calculated lattice constants *a* and *c* of bulk MoS₂ are 3.191 and 12.374 Å. They are slightly larger (1%) than the values of experiments (3.160 and 12.295 Å). This small overestimate of the lattice constants with the PBE functional is not significant for our analysis about the effects of pressure on the electronic structure. We note that smaller lattice parameters could be obtained using the PBEsol functional if needed.^{51,52} For the different layered MoS₂, the supercells are constructed with a vacuum space of 20 Å along *z* direction. The Brillouin zones are sampled with the Γ -centered *k*-point grid of 18 × 18 × 1. For single-layer MoS₂, the structure has the hexagonal symmetry with space group $P\bar{6}m2$. There are six sulfur atoms near each Mo atom to form a trigonal prismatic structure with the mirror symmetry in *z* direction. The resulting crystal field splitting yields band structures around the gap derived mainly from Mo *d*-electron orbitals. The vdW interaction is important in the adhesion of the layers to form the bulk. The stacking can be understood in terms of attractive Coulomb interactions between sulfur atoms and Mo atoms and Coulomb and closed shell repulsion between sulfur atoms in adjacent layers. The net result is AB-stacking. This results in the sulfur atoms of second-layer on the hexagonal center of first-layer and the Mo atoms on the top of first-layer sulfur atoms.

As mentioned, Mo *d* states form the band edges. For each layer, the Mo atoms are located in the center of layer for *z* direction. Therefore, direct interactions between orbitals of Mo atoms from different layers will be very weak. The method for applying pressure in the present calculations was to add external stress to stress tensor in VASP code,^{35–37} and the structure of bulk MoS₂ was then optimized under a specified hydrostatic pressure. We calculated the structural change of bulk MoS₂ under different pressures up to 25 GPa. We then used these structural parameters from bulk MoS₂ to construct single-, double- and three-layer MoS₂ structures corresponding to different pressures.

3. RESULTS AND DISCUSSION

3.1. Electronic Structures of MoS₂ with Different Number of Layers.

The band structures of single-layer, double-layer, three-layer and bulk MoS₂ are shown in Figure 1.

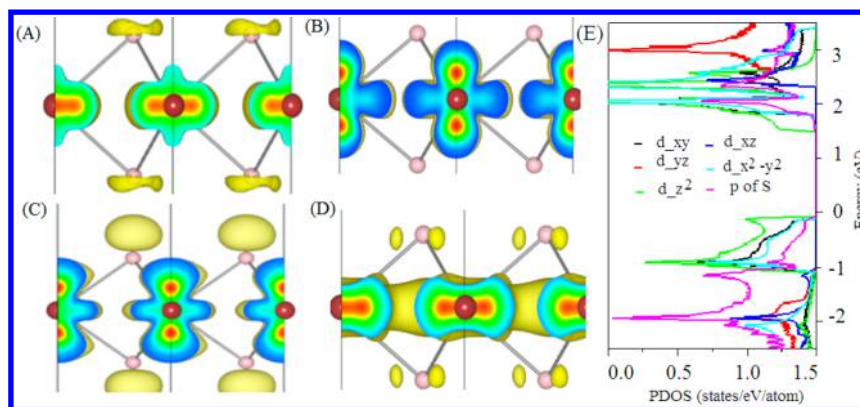


Figure 2. Isosurfaces of band-decomposed charge density at BCB- Λ (A), BCB-K (B), TVB- Γ (C), and TVB-K (D) and partial density of states of Mo and S atoms (E) of single-layer MoS₂. Notice that Λ point is a k point along the direction $\Gamma \rightarrow K$ with an energy minimum in conduction band as shown in Figure 1A.

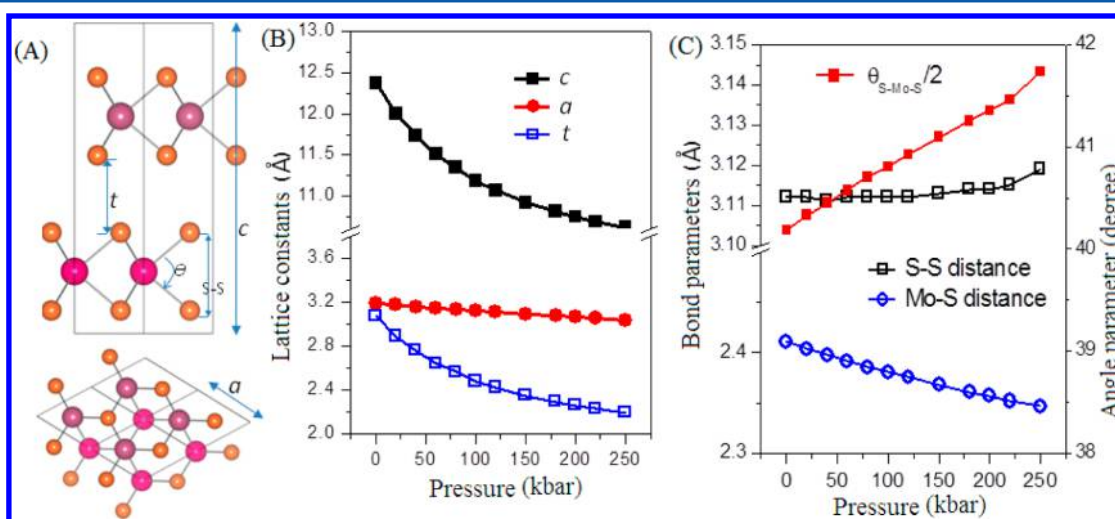


Figure 3. Structure (A) and change of lattice constants, bond parameters, and angle parameter under pressure (B and C) of AB-stacked bulk MoS₂.

The results are consistent with the previous theoretical studies.²⁰ The band gap at the K point, which is related to the direct excitonic transition in the experimental observations (two exciton absorption peaks at about 1.85 and 1.98 eV due to the spin–orbital coupling), is barely changed with increasing numbers of layers. On the other hand, the indirect band gap between the Γ point and K/ Λ point decreases. This results in a crossover between an indirect gap and a direct gap. There is generally a very high intraband relaxation rate for electrons or holes in a semiconductor. Therefore, this crossover and specifically the change in band ordering between may result in weakness or nonobservation of the luminescence associated with these excitons. In addition, it may be seen that the direct band gap at Γ decreases with increasing number of layers due to the change of energy position of TVB (Figure 1). For multilayer and bulk MoS₂, the direct gap at Γ is less than that at K. This will decrease the absorption efficiency at the K point due to the competition from Γ . Therefore, the photoluminescence ratio at K for multilayer MoS₂ will be depressed as observed in experiments.

The unusual variation of the band structure with number of layers can be ascribed to the characteristics of the Mo d orbitals comprising the different states near band gap. In Figure 2, the isosurfaces of band-decomposed charge densities at BCB of Λ point (BCB- Λ), BCB of K point (BCB-K), TVB of Γ point

(TVB- Γ), and TVB of K point (TVB-K) with partial density of states of Mo and S atoms are shown. The state at BCB- Λ is mainly of d_{xy} and $d_{x^2-y^2}$ character, while that at the K of TVB has $d_{x^2-y^2}$ character. The states at BCB-K and TVB- Γ are mainly d_z^2 derived. In addition, it is seen that there is noticeable charge on the top of sulfur atoms (p_z) for the states at BCB- Λ and TVB- Γ . This is not the case for the state at TVB-K. Therefore, the coupling of layers will result in a large splitting of band states at BCB- Λ and TVB- Γ , while the splitting of the energy states at BCB-K and TVB-K will be small, simply reflecting the different orbital characters. This explains the change of band structures with the increasing number of layers.

3.2. Bulk MoS₂ under Pressure. The structure of bulk MoS₂ responds to pressure in an anisotropic way. As shown in Figure 3, the lattice constant c and the parameter t for the distance between two layers decreases strongly under pressure, reflecting the fact that the interlayer bonding is associated with weak vdW interactions. The in-plane lattice constant a is much more weakly affected by pressure. It is also found that the thickness of a single layer of MoS₂ defined by the S–S distance increases slightly under pressure while the length of the Mo–S bonds is decreased. This results in increase of the bond angle θ under pressure. As mentioned, the charge distributions of the different states around band gap have the different spatial distributions, reflecting their orbital characters. The partial

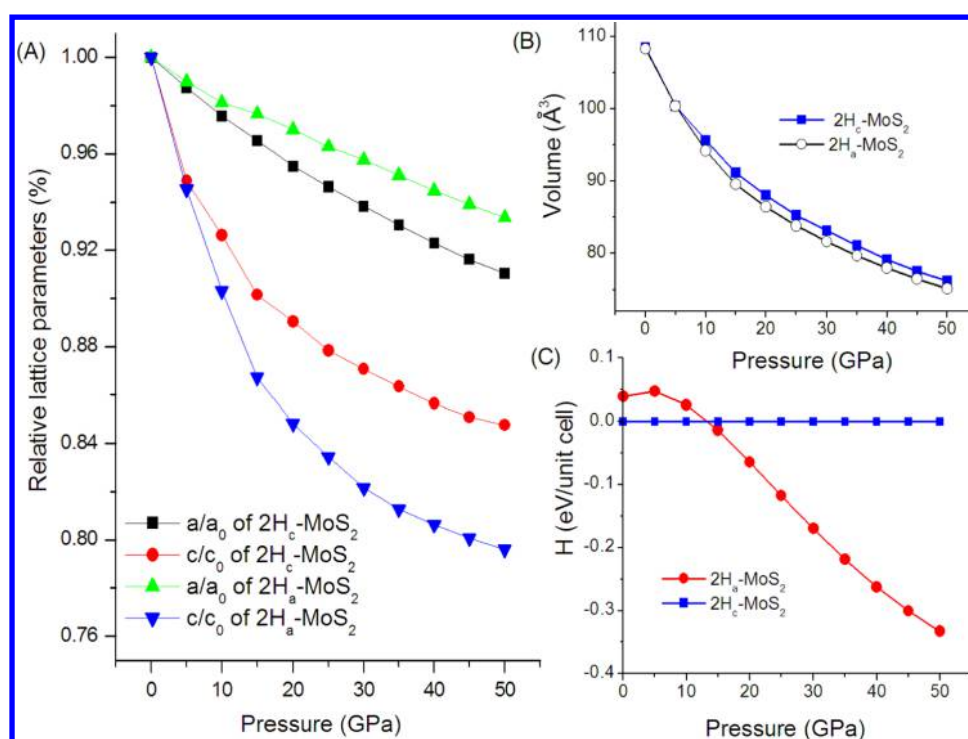


Figure 4. Calculated relative lattice parameters, volumes, and relative enthalpies of $2H_c$ - and $2H_a$ - MoS_2 structures as a function of pressure. The lattice parameters are referenced to their equilibrium values under zero pressure (corresponding to 100%). The lattice constants a_0 and c_0 of $2H_a$ - MoS_2 are 3.193 and 12.271 Å, respectively.

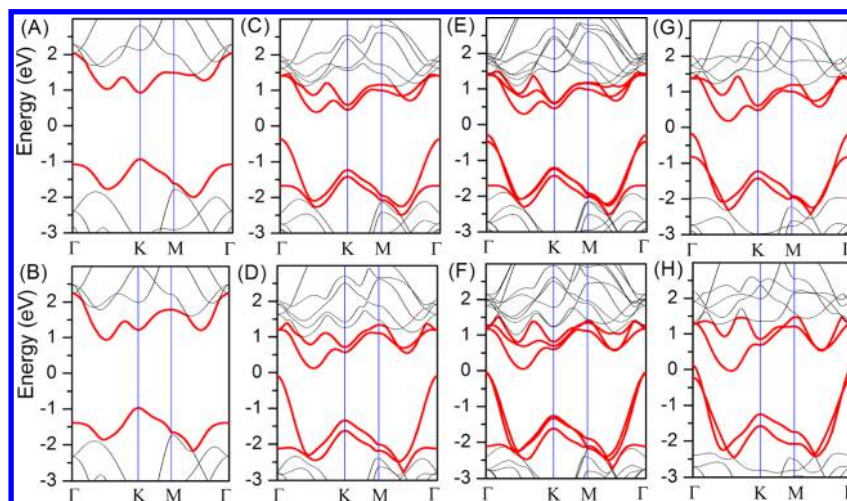


Figure 5. Band structures of single-layer (A, B), double-layer (C, D), three-layer (E, F), and bulk MoS_2 (G, H) under the pressure of 100 and 250 kbar.

density of states (PDOS, Figure 2E) shows that the energy bands of mixed Mo–S character are located in the occupied bands below the valence band edge. This is a nominally S^{2-} configuration, hybridized with the nominally tetravalent Mo. With this configuration it would not be surprising for the bond angle to also modulate the band structures under pressure.

We note that under pressure it is possible that there is a phase transition from the $2H_c$ phase to $2H_a$ phase for bulk MoS_2 . For the usual $2H_c$ phase, the two Mo atoms occupy the sites b ($1/3, 2/3, 1/4$) and c ($2/3, 1/3, 3/4$). The relative movement between two layers in one unit cell in x - y plane will yield the transition from $2H_c$ to $2H_a$ if the Mo atom on the site b moves to the site ($2/3, 1/3, 1/4$) or that on the site c moves

to the site ($1/3, 2/3, 3/4$). Recently, the experiment results reported by Bandaru et al. indicate this isostructural transition on MoS_2 may occur at high pressure.³⁰ We calculated the cell parameters and relative enthalpies of $2H_c$ - and $2H_a$ - MoS_2 under different pressures, as shown in Figure 4. The volume of $2H_c$ is larger than that of $2H_a$ under the pressure, but the difference is small (Figure 4B). The change of volume under pressure is consistent with the experimental results of Bandaru et al. The change of lattice parameters of $2H_a$ is also consistent with the experimental results. In addition the difference in lattice parameters of these phases increases pressure, especially the lattice parameter c . We also calculated the change of lattice parameter without considering dispersion interactions (Figure

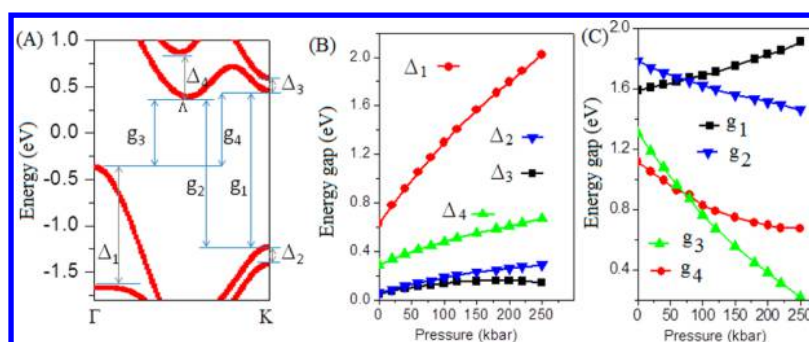


Figure 6. Band structure of double-layer MoS₂ under 100 kbar (A) and change of band parameters (B) and gaps (C) of double-layer MoS₂ with the pressure.

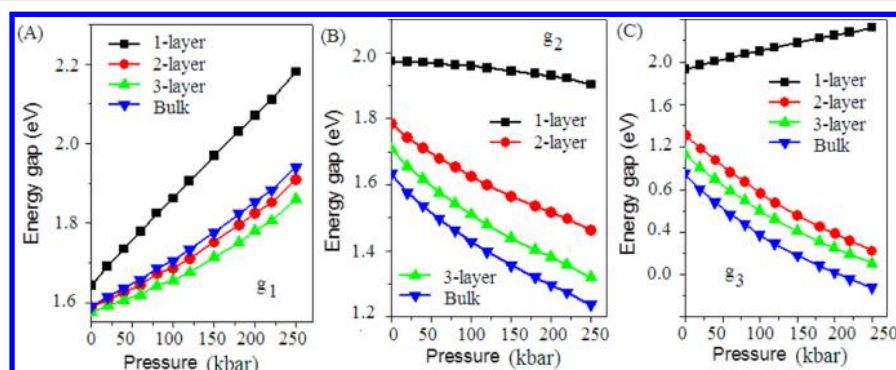


Figure 7. Change of gap g_1 (A), g_2 (B), and g_3 (C) of single-layer, double-layer, three-layer, and bulk MoS₂ under pressure. Notice the gaps are defined following the way of that of the double-layer in Figure 5A.

S1 of the Supporting Information), and in this case the variation of the lattice parameters with pressure is inconsistent with the results of Bandaru et al. This reflects the fact that vdW interactions are important for the interlayer interactions, even at high pressure. On the other hand, zero-point energy and entropic contributions can be neglected in the relative stability of the phases, since these two phases are very similar from a local structural and bonding point of view. The $2H_c$ and $2H_a$ enthalpies cross near 13 GPa (Figure 4C). This means $2H_a$ phase is more stable above 13 GPa. The experimental results indicated the new phase began to emerge from the parent structure $2H_c$ around 17 GPa. The small difference between theoretical and experimental results may be due to the nonhydrostatic experimental pressure and high dynamical potential barrier or density functional errors in the present calculation. In any case, this phase is stabilized at high pressure due to a higher compressibility as indicated by the variation of the lattice parameters.

The band structures of double-layer and bulk $2H_a$ -MoS₂ were calculated (Figure S2 of the Supporting Information), and were found to be similar to those of $2H_c$ -MoS₂ (Figure 1). While MoS₂ is known to exhibit different polytypes, this does seem to be unimportant in the main features of the band structure under pressure. We studied two structures from among the polymorphs of MoS₂ and calculated the band structures (Figure S3 of the Supporting Information), but do not find substantial differences other than the lifting of degeneracies due to layers coupling in folded reciprocal lattice cells. Thus, stacking faults do modify the electronic structure, but only weakly.

3.3. Electronic Properties of MoS₂ under Pressure. The band structures of single-layer MoS₂ at pressures of 100 kbar and 250 kbar are shown in Figure 5A and B. The energy of the

state at BCB- Λ relative to that at BCB-K point decreases with increasing pressure. The energy of the state at TVB-K relative to that at TVB- Γ is increased. The state at BCB- Λ and that at TVB-K can be considered to be as a pair of bonding and antibonding states with mainly $d_{x^2-y^2}$ character. The state at BCB-K and that at TVB- Γ are a pair of states with mainly d_z^2 character. With the increase of bond angle under pressure, the coupling between the states with the $d_{x^2-y^2}$ character and those from the Mo-S bond will weaken. This results in a decrease of band energy splitting of the pairs of states at BCB- Λ and TVB-K. In contrast, the coupling between the states of d_z^2 character and that from the Mo-S bond will strengthen. The energy splitting of pair of states at BCB-K and TVB- Γ will increase. Finally, with increase of pressure, the energy position of state at BCB- Λ will be lower than that at BCB-K. The band gap of single layer MoS₂ will thus change from direct to indirect and the photoluminescence will weaken.

The situation for multilayer and bulk MoS₂ is complicated by the coupling between the layers. As shown in Figure 5C-H, the effect of the layering seems to be more important than the bond angle effect. This is because the change of the distance between layers is very strong under pressure. We discuss bilayer MoS₂ in detail to illustrate this. The important parameters with the pressure are shown in Figure 6. The four important states (at TVB- Γ , TVB-K, BCB- Λ , and BCB-K), which are related to the band gap, are split due to the coupling between the layers. The widths of band splitting represented by the parameters Δ_1 , Δ_2 , Δ_3 , and Δ_4 have increased under pressure. The splitting width Δ_1 is the largest of the four parameters. This can be understood in terms of the orbital character, specifically the hybridization with the S p_z states pointing to the next layer. The change of different band gaps for the MoS₂ with different

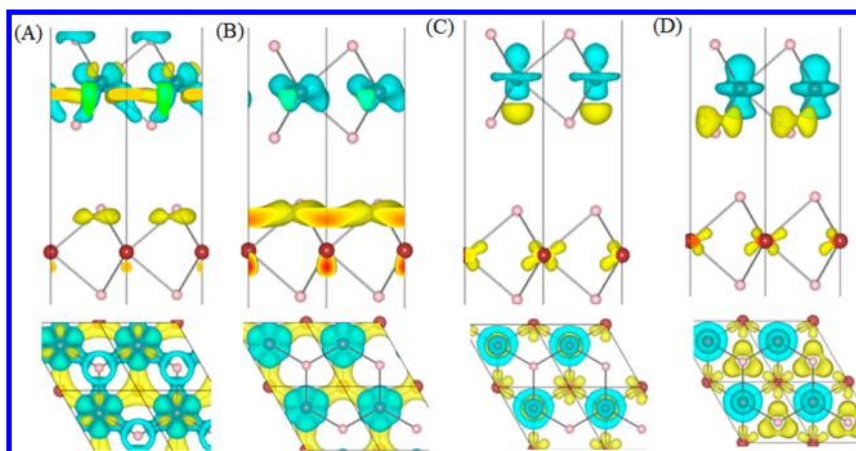


Figure 8. Charge difference isosurfaces of band-decomposed charge density of double-layer MoS₂ at TVB-K with respect to that of single-layer MoS₂ which is the up-layer of double-layer MoS₂ under 0 kbar (A) and 200 kbar (B) and that of band-decomposed charge density of double-layer MoS₂ at BCB-K with respect to that of single-layer MoS₂ which is the up-layer of double-layer MoS₂ under 0 kbar (C) and 200 kbar (D) (yellow color for charge accumulation, and blue color for charge depletion).

numbers of layers is depicted in detail in Figure 7. The direct band gap (g_1) at K point increases with pressure. This can be attributed to the shortening of the bond length, similar to the observed in the most semiconductors. The change of g_1 is largest for the single-layer case, and can be attributed to the increase of band splitting at BCB-K and TVB-K with the pressure. It is interesting that the g_1 of bulk MoS₂ is larger than that of multilayered MoS₂ cases studied. This may be due to the breaking of layers' stacking period in z direction and the absence of periodic interaction of layers in multilayer. For the g_2 and g_3 of multilayer and bulk, there is a decrease under pressure. This is due to the large band splitting at BCB- Λ and TVB- Γ . Therefore, the change of band structures of multilayer and bulk MoS₂ under pressure is controlled mostly by the coupling of layers.

Insight into the effect of layer coupling, which results in the band splitting at BCB- Λ , BCB-K, TVB- Γ , and TVB-K under pressure, can be obtained from the changes of charge distribution of the four states. The results for double-layer are shown in Figure 8 and Figure 9. It is found that the charge of the states at TVB and BCB of K point are mostly from the top layer (second layer) of double layers. In Figure 8, the charge difference isosurface of band-decomposed charge density is defined by the formula,

$$\Delta\text{BDChg}(r) = \text{BDChg}_{2\text{-layer}}(r) - \text{BDChg}_{2\text{nd-layer}}(r) \quad (1)$$

where $\text{BDChg}_{2\text{-layer}}(r)$ and $\text{BDChg}_{2\text{nd-layer}}(r)$ are the charge density of an energy state at a particular \mathbf{k} -point of the double-layer MoS₂ and the charge density of the corresponding energy state of the isolated single layer MoS₂, respectively. The coupling of like states of the two layers will lead to charge redistribution. However, as seen for the states at TVB-K and BCB-K, the coupling is weak and the splitting of states (Δ_2 and Δ_3) is small. As an example, the charge redistribution of one of two split states at TVB-K is shown in Figure 8A. With the pressure (Figure 8B and D), much more charge is transferred to the first layer for the state at TVB-K and much more charge is redistributed on the sulfur atoms of the same layer for the state at BCB-K. This may be used to explain why the change of Δ_2 is larger than that of Δ_3 under the pressure.

For the states at TVB- Γ and BCB- Λ , the changes are found to be mainly from the contributions of both layers. In Figure 9,

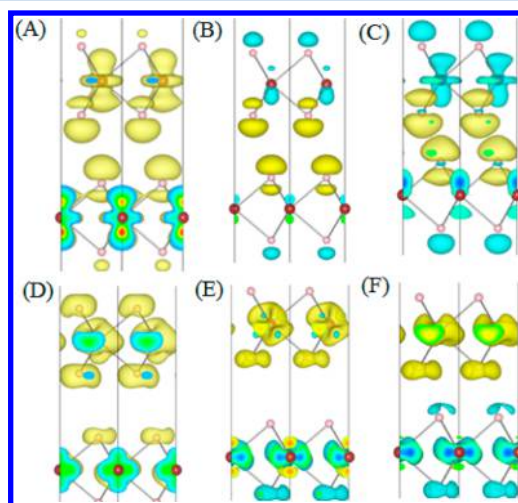


Figure 9. Isosurfaces of band-decomposed charge density at TVB- Γ (A) and BCB- Λ (D), and charge difference isosurfaces of band-decomposed charge density of double-layer MoS₂ at TVB- Γ with respect to the half of charge density of both single-layer MoS₂ under 0 kbar (B) and 200 kbar (C) and that of band-decomposed charge density of double-layer MoS₂ at BCB- Λ with respect to the half of charge density of both single-layer MoS₂ under 0 kbar (E) and 200 kbar (F) (yellow color for charge accumulation, and blue color for charge depletion in B, C, E and F).

the difference isosurface of band-decomposed charge density is defined by the formula,

$$\Delta\text{BDChg}(r) = \text{BDChg}_{2\text{-layer}}(r) - \frac{1}{2}\text{BDChg}_{2\text{nd-layer}}(r) - \frac{1}{2}\text{BDChg}_{1\text{st-layer}}(r) \quad (2)$$

where $\text{BDChg}_{2\text{-layer}}(r)$, $\text{BDChg}_{2\text{nd-layer}}(r)$ and $\text{BDChg}_{1\text{st-layer}}(r)$ are the charge density of an energy state at a particular \mathbf{k} point for double-layer MoS₂ and the charge densities of the corresponding energy states of the second isolated single layer MoS₂ and the first isolated single layer MoS₂, respectively. Obviously, the strong coupling of both layers and the charge redistribution result in the large splitting of states at TVB- Γ and BCB- Λ . This is the reason that Δ_1 and Δ_4 are larger than Δ_2 and Δ_3 . Under pressure, there are more charges transferred to

the sulfur atoms of both layers for the state at Γ of TVB. This may be reason that the change of Δ_1 under the pressure is the largest of the four splitting widths.

4. CONCLUSIONS

We used first-principles calculations to study the changes in electronic structure of single and multilayer MoS₂ under pressure. The band gap of the single-layer can be changed from direct to indirect under pressure. Multilayer MoS₂ is more easily changed from semiconductor to metal under pressure. The metallization of multilayer MoS₂ under pressure can be attributed to the increase of band splitting at TVB- Γ and BCB- Λ due to the strong redistribution of charge for both states. The change of the relative energies of the four special states (at BCB- Λ , BCB-K, TVB- Γ , and TVB-K) under pressure can be attributed to the different orbital character of the four states and bond angle effect for single-layer MoS₂. Similarly, the effect of bond angle is important for the band structure changes under the tensile strain, which has been studied experimentally. Finally, the variation of the layer separation modulates the band structure strongly, perhaps sufficiently strongly to modulate the luminescence under readily achievable conditions.

■ ASSOCIATED CONTENT

Supporting Information

Figures showing calculated relative lattice parameters, volumes, and relative enthalpies of $2H_a$ - and $2H_c$ -MoS₂ structures as a function of pressure; structure and band structures of double-layer and bulk $2H_a$ -MoS₂ without considering van der Waals interaction; structures of two polymorphs of $2H_c$ -MoS₂ and band structures of A structure and C structure. The Supporting Information is available free of charge on the ACS Publications website at DOI: 10.1021/acs.jpcc.5b00317.

■ AUTHOR INFORMATION

Corresponding Authors

*E-mail: xffan@jlu.edu.cn. Tel: +86-8516-8444.

*E-mail: singhdj@ornl.gov. Tel: 865-241-1944.

Notes

The authors declare no competing financial interest.

■ REFERENCES

- (1) Novoselov, K. S.; Geim, A. K.; Morozov, S. V.; Jiang, D.; Zhang, Y.; Dubonos, S. V.; Grigorieva, I. V.; Firsov, A. A. Electric Field Effect in Atomically Thin Carbon Films. *Science* **2004**, *306*, 666–669.
- (2) Geim, A. K.; Novoselov, K. S. The Rise of Graphene. *Nat. Mater.* **2007**, *6*, 183–191.
- (3) Stoller, M. D.; Park, S.; Zhu, Y.; An, J.; Ruoff, R. S. Graphene-Based Ultracapacitors. *Nano Lett.* **2008**, *8*, 3498–3502.
- (4) Fan, X.; Zheng, W. T.; Kuo, J.-L. Adsorption and Diffusion of Li on Pristine and Defective Graphene. *ACS Appl. Mater. Interfaces* **2012**, *4*, 2432–2438.
- (5) Mak, K. F.; Lee, C.; Hone, J.; Shan, J.; Heinz, T. F. Atomically Thin MoS₂: A New Direct-Gap Semiconductor. *Phys. Rev. Lett.* **2010**, *105*, 136805.
- (6) Lee, C.; Yan, H.; Brus, L. E.; Heinz, T. F.; Hone, J.; Ryu, S. Anomalous Lattice Vibrations of Single- and Few-Layer MoS₂. *ACS Nano* **2010**, *4*, 2695–2700.
- (7) Novoselov, K. S.; Jiang, D.; Schedin, F.; Booth, T. J.; Khotkevich, V. V.; Morozov, S. V.; Geim, A. K. Two-Dimensional Atomic Crystals. *Proc. Natl. Acad. Sci. U. S. A.* **2005**, *102*, 10451–10453.
- (8) Splendiani, A.; Sun, L.; Zhang, Y.; Li, T.; Kim, J.; Chim, C.-Y.; Galli, G.; Wang, F. Emerging Photoluminescence in Monolayer MoS₂. *Nano Lett.* **2010**, *10*, 1271–1275.

- (9) Wang, Q. H.; Kalantar-Zadeh, K.; Kis, A.; Coleman, J. N.; Strano, M. S. Electronics and Optoelectronics of Two-Dimensional Transition Metal Dichalcogenides. *Nat. Nanotechnol.* **2012**, *7*, 699–712.
- (10) Mattheiss, L. F. Band Structures of Transition-Metal-Dichalcogenide Layer Compounds. *Phys. Rev. B* **1973**, *8*, 3719–3740.
- (11) Kibsgaard, J.; Chen, Z.; Reinecke, B. N.; Jaramillo, T. F. Engineering the Surface Structure of MoS₂ to Preferentially Expose Active Edge Sites for Electrocatalysis. *Nat. Mater.* **2012**, *11*, 963–969.
- (12) Radisavljevic, B.; Radenovic, A.; Brivio, J.; Giacometti, V.; Kis, A. Single-Layer MoS₂ Transistors. *Nat. Nanotechnol.* **2011**, *6*, 147–150.
- (13) Yoon, Y.; Ganapathi, K.; Salahuddin, S. How Good Can Monolayer MoS₂ Transistors Be? *Nano Lett.* **2011**, *11*, 3768–3773.
- (14) Xiao, D.; Liu, G.-B.; Feng, W.; Xu, X.; Yao, W. Coupled Spin and Valley Physics in Monolayers of MoS₂ and Other Group-VI Dichalcogenides. *Phys. Rev. Lett.* **2012**, *108*, 196802.
- (15) Yao, W.; Xiao, D.; Niu, Q. Valley-Dependent Optoelectronics from Inversion Symmetry Breaking. *Phys. Rev. B* **2008**, *77*, 235406.
- (16) Kuc, A.; Zibouche, N.; Heine, T. Influence of Quantum Confinement on the Electronic Structure of the Transition Metal Sulfide TS₂. *Phys. Rev. B* **2011**, *83*, 245213.
- (17) Zeng, H.; Liu, G.-B.; Dai, J.; Yan, Y.; Zhu, B.; He, R.; Xie, L.; Xu, S.; Chen, X.; Yao, W.; Cui, X. Optical Signature of Symmetry Variations and Spin-Valley Coupling in Atomically Thin Tungsten Dichalcogenides. *Sci. Rep.* **2013**, *3*, 1608.
- (18) Sundaram, R. S.; Engel, M.; Lombardo, A.; Krupke, R.; Ferrari, A. C.; Avouris, P.; Steiner, M. Electroluminescence in Single Layer MoS₂. *Nano Lett.* **2013**, *13*, 1416–1421.
- (19) Feng, J.; Qian, X.; Huang, C.-W.; Li, J. Strain-Engineered Artificial Atom as a Broad-Spectrum Solar Energy Funnel. *Nat. Photonics* **2012**, *6*, 866–872.
- (20) Yun, W. S.; Han, S. W.; Hong, S. C.; Kim, I. G.; Lee, J. D. Thickness and Strain Effects on Electronic Structures of Transition Metal Dichalcogenides: 2H-MX₂ Semiconductors (M = Mo, W; X = S, Se, Te). *Phys. Rev. B* **2012**, *85*, 033305.
- (21) Johari, P.; Shenoy, V. B. Tuning the Electronic Properties of Semiconducting Transition Metal Dichalcogenides by Applying Mechanical Strains. *ACS Nano* **2012**, *6*, 5449–5456.
- (22) Bhattacharyya, S.; Singh, A. K. Semiconductor-Metal Transition in Semiconducting Bilayer Sheets of Transition-Metal Dichalcogenides. *Phys. Rev. B* **2012**, *86*, 075454.
- (23) Lu, P.; Wu, X.; Guo, W.; Zeng, X. C. Strain-Dependent Electronic and Magnetic Properties of MoS₂ Monolayer, Bilayer, Nanoribbons and Nanotubes. *Phys. Chem. Chem. Phys.* **2012**, *14*, 13035–13040.
- (24) Fan, X.; Zheng, W.; Kuo, J.-L.; Singh, D. J. Structural Stability of Single-layer MoS₂ under Large Strain. *J. Phys.: Condens. Matter* **2015**, *27*, 105401.
- (25) Scalise, E.; Houssa, M.; Pourtois, G.; Afanasev, V.; Stesmans, A. Strain-Induced Semiconductor to Metal Transition in the Two-Dimensional Honeycomb Structure of MoS₂. *Nano Res.* **2012**, *5*, 43–48.
- (26) Conley, H. J.; Wang, B.; Ziegler, J. I.; Haglund, R. F.; Pantelides, S. T.; Bolotin, K. I. Bandgap Engineering of Strained Monolayer and Bilayer MoS₂. *Nano Lett.* **2013**, *13*, 3626–3630.
- (27) Webb, A. W.; Feldman, J. L.; Skelton, E. F.; Towle, L. C.; Liu, C. Y.; Spain, I. L. High Pressure Investigations of MoS₂. *J. Phys. Chem. Solids* **1976**, *37*, 329–335.
- (28) Aksoy, R.; Ma, Y.; Selvi, E.; Chyu, M. C.; Ertas, A.; White, A. X-ray Diffraction Study of Molybdenum Disulfide to 38.8 GPa. *J. Phys. Chem. Solids* **2006**, *67*, 1914–1917.
- (29) Hromadova, L.; Martonak, R.; Tosatti, E. Structure Change, Layer Sliding, and Metallization in High-Pressure MoS₂. *Phys. Rev. B* **2013**, *87*, 144105.
- (30) Bandaru, N.; Kumar, R. S.; Sneed, D.; Tschauner, O.; Baker, J.; Antonio, D.; Luo, S.-N.; Hartmann, T.; Zhao, Y.; Venkat, R. Effect of Pressure and Temperature on Structural Stability of MoS₂. *J. Phys. Chem. C* **2014**, *118*, 3230–3235.

- (31) Duerloo, K.-A. N.; Li, Y.; Reed, E. J. Structural Phase Transitions in Two-Dimensional Mo- and W-Dichalcogenide Monolayers. *Nat. Commun.* **2014**, *5*, 4214.
- (32) Peelaers, H.; Van de Walle, C. G. Elastic Constants and Pressure-Induced Effects in MoS₂. *J. Phys. Chem. C* **2014**, *118*, 12073–12076.
- (33) Guo, H.; Yang, T.; Tao, P.; Wang, Y.; Zhang, Z. High Pressure Effect on Structure, Electronic Structure, and Thermoelectric Properties of MoS₂. *J. Appl. Phys.* **2013**, *113*, 013709.
- (34) Dou, X.; Ding, K.; Jiang, D.; Sun, B. Tuning and Identification of Interband Transitions in Monolayer and Bilayer Molybdenum Disulfide Using Hydrostatic Pressure. *ACS Nano* **2014**, *8*, 7458–7464.
- (35) Hohenberg, P.; Kohn, W. Inhomogeneous Electron Gas. *Phys. Rev.* **1964**, *136*, B864–B871.
- (36) Kresse, G.; Furthmüller, J. Efficient Iterative Schemes for Ab Initio Total-Energy Calculations Using a Plane-wave Basis Set. *Phys. Rev. B* **1996**, *54*, 11169–11186.
- (37) Kresse, G.; Furthmüller, J. Efficiency of Ab-Initio Total Energy Calculations for Metals and Semiconductors Using a Plane-wave Basis Set. *Comput. Mater. Sci.* **1996**, *6*, 15–50.
- (38) Perdew, J. P.; Burke, K.; Ernzerhof, M. Generalized Gradient Approximation Made Simple. *Phys. Rev. Lett.* **1996**, *77*, 3865–3868.
- (39) Grimme, S. Semiempirical GGA-Type Density Functional Constructed with a Long-Range Dispersion Correction. *J. Comput. Chem.* **2006**, *27*, 1787–1799.
- (40) Fan, X. F.; Zheng, W. T.; Chihai, V.; Shen, Z. X.; Kuo, J.-L. Interaction Between Graphene and the Surface of SiO₂. *J. Phys.: Condens. Matter* **2012**, *24*, 305004.
- (41) Mercurio, G.; McNellis, E. R.; Martin, I.; Hagen, S.; Leyssner, F.; Soubatch, S.; Meyer, J.; Wolf, M.; Tegeder, P.; Tautz, F. S.; Reuter, K. Structure and Energetics of Azobenzene on Ag(111): Benchmarking Semiempirical Dispersion Correction Approaches. *Phys. Rev. Lett.* **2010**, *104*, 036102.
- (42) Qiu, D. Y.; da Jornada, F. H.; Louie, S. G. Optical Spectrum of MoS₂: Many-Body Effects and Diversity of Exciton States. *Phys. Rev. Lett.* **2013**, *111*, 216805.
- (43) Ramasubramaniam, A. Large Excitonic Effects in Monolayers of Molybdenum and Tungsten Dichalcogenides. *Phys. Rev. B* **2012**, *86*, 115409.
- (44) Komsa, H.-P.; Krasheninnikov, A. V. Effects of Confinement and Environment on the Electronic Structure and Exciton Binding Energy of MoS₂ from First Principles. *Phys. Rev. B* **2012**, *86*, 241201.
- (45) Shi, H.; Pan, H.; Zhang, Y.-W.; Yakobson, B. I. Quasiparticle Band Structures and Optical Properties of Strained Monolayer MoS₂ and WS₂. *Phys. Rev. B* **2013**, *87*, 155304.
- (46) Molina-Sanchez, A.; Sangalli, D.; Hummer, K.; Marini, A.; Wirtz, L. Effect of Spin-Orbit Interaction on the Optical Spectra of Single-Layer, Double-Layer, and Bulk MoS₂. *Phys. Rev. B* **2013**, *88*, 045412.
- (47) Liu, G. B.; Shan, W. Y.; Yao, Y.; Xiao, D. Three-Band Tight-Binding Model for Monolayers of Group-VIB Transition metal Dichalcogenides. *Phys. Rev. B* **2013**, *88*, 085433.
- (48) Cappelluti, E.; Roldán, R.; Silva-Guillén, J. A.; Ordejón, P.; Guinea, F. Tight-Binding Model and Direct-Gap/Indirect-Gap Transition in Single-Layer and Multilayer MoS₂. *Phys. Rev. B* **2013**, *88*, 075409.
- (49) Koskinen, P.; Fampiou, I.; Ramasubramaniam, A. Density-Functional Tight-Binding Simulations of Curvature-Controlled Layer Decoupling and Band-Gap Tuning in Bilayer MoS₂. *Phys. Rev. Lett.* **2014**, *112*, 186802.
- (50) Zahid, F.; Liu, L.; Zhu, Y.; Wang, J.; Guo, H. A Generic Tight-Binding Model for Monolayer, Bilayer and Bulk MoS₂. *AIP Adv.* **2013**, *3*, 052111.
- (51) Perdew, J. P.; Ruzsinszky, A.; Csonka, G. I.; Vydrov, O. A.; Scuseria, G. E.; Constantin, L. A.; Zhou, X.; Burke, K. Restoring the Density-Gradient Expansion for Exchange in Solids and Surfaces. *Phys. Rev. Lett.* **2008**, *100*, 136406.
- (52) Perdew, J. P.; Ruzsinszky, A.; Csonka, G. I.; Vydrov, O. A.; Scuseria, G. E.; Constantin, L. A.; Zhou, X.; Burke, K. Erratum: